

# How Hot should Glass Get?

## Comparing Thermal Loading Criteria in Spandrel Glass

Terrence R. McDonnell <sup>a</sup>, David E. Kosnik <sup>a</sup>, Richard Green <sup>b</sup>, Andrew Crosby <sup>c</sup>

- a CTLGroup, Mount Prospect, IL. USA, [tmcdonnell@ctlgroup.com](mailto:tmcdonnell@ctlgroup.com), [dkosnik@ctlgroup.com](mailto:dkosnik@ctlgroup.com)
- b Green Facades, Mountlake Terrace, WA. USA, [richard@greenfacadesllc.com](mailto:richard@greenfacadesllc.com)
- c Read Jones Christoffersen, ON. CAN, [acrosby@rjc.ca](mailto:acrosby@rjc.ca)

### Abstract

This paper presents various methodologies for calculating the temperature differential in glass spandrel panels. Some methodologies have been derived from direct measurements in case studies. Others from international standards or research papers. As energy codes for buildings continue to demand more efficiency within the exterior walls of buildings gradually, the ‘we always did it this way’ approaches will no longer work and may potentially lead to unsafe conditions for spandrel glass. Spandrel glass was developed to preserve a continuous glazing aesthetic while covering the perimeter structure with glass coatings and a layer of insulation directly behind the glass, which is not visible. While this makeup provides benefits, such as reducing the overall u-value of the exterior wall system, it often does so by significantly increasing the temperature differential across the glass surface. When this temperature difference is not accounted for, spandrel glass is often prone to fracture. Fractures have become common enough in the construction industry that the National Glass Association has published technical notes to educate the building design and construction community about the phenomenon. In this paper, we present various methodologies for predicting the design surface temperature of glass and compare them with forensic data we gathered from a building’s spandrel panel with a history of thermal fracture. We conclude the paper with our recommendation of the thermal temperature determination process that a design team can use to address this phenomenon responsibly.

### Keywords

Glass, Spandrel, Temperature, Thermal

### Article Information

- Digital Object Identifier (DOI): [10.47982/cgc.10.745](https://doi.org/10.47982/cgc.10.745)
- Published by [Challenging Glass](#), on behalf of the author(s), at [Stichting OpenAccess](#).
- Published as part of the peer-reviewed [Challenging Glass Conference Proceedings](#), Volume 10, June 2026, [10.47982/cgc.10](https://doi.org/10.47982/cgc.10)
- Editors: Christian Louter, Freek Bos & Jan Belis
- This work is licensed under a [Creative Commons Attribution 4.0 International](#) (CC BY 4.0) license.
- Copyright © 2026 with the author(s)

## 1. Introduction

Exterior wall systems offer a unique area of study within the design and construction of buildings. They often sit at the intersection of material science, building physics, climate science, structural engineering, and architectural engineering. This combination of demands often requires multiple building design and construction standards to achieve the desired design goal.

### 1.1. Historical Perspective

Energy-efficiency goals have given rise to and continue to influence the development and deployment of innovative exterior wall systems. One such influential document is ASHRAE 90.1 (the ANSI/ASHRAE/IES Standard 90.1: Energy Standard for Buildings Except Low-Rise Residential Buildings). ASHRAE 90.1 was developed in response to the energy crisis in the United States during the 1970s. In the early 1980s, ASHRAE set a goal to reduce the energy use of the new building stock by 100% compared to the 1970s. One result of this gradual, ongoing tightening of building code energy requirements is an increase in the overall insulation performance (U-value) of the exterior wall system for all buildings, alongside increased energy efficiency of building systems. The U-value is the rate at which a window transmits non-solar heat flow, according to the United States Department of Energy and NFRC (National Fenestration Rating Council 100 Standard). For large buildings that use glass and glazing systems, this led to the incorporation of spandrel panels within the modern curtainwall systems.

### 1.2. Glass Spandrel Panels – Nomenclature, Purpose, and Significance

Simply put, a spandrel panel is a glass panel composed of the same glass makeup as a building's vision glass and includes the following two items:

1. A type of coating (usually on the innermost surface of the glass makeup) that visible light either barely transmits through, or not at all, making the overall glass panel opaque. The most common coatings are composed of either ceramic frit or silicone elastomeric paint.
2. A layer of insulation behind the coating that will compensate for the lower-performing vision glass portions of the building, thus improving the overall insulating value of the exterior wall system as a whole.

These two items allow the spandrel panel to fulfill its purpose;

1. Conceal an undesired item from vision, such as perimeter beams, slab edges, or columns, while maintaining a continuous glass exterior surface aesthetic.
2. Improve the overall thermal insulation value (U-Value) of the building exterior by incorporating thick portions of insulation behind the opaque layer of the panel.

In modern buildings, both spandrel panels and vision glass are typically composed of insulated glass units (IGUs). An IGU consists of an airtight assembly of two (or more) lites of glass separated by an inert gas. Glass surfaces are numbered from outside to inside; thus, for a two-lite IGU, Surface No. 1 is the outer surface of the outer lite (i.e., the exterior of the building, and Surface No. 4 is the inside face of the inner lite (for a double glazing monolithic system), closest to the interior of the building. (Figure 1).

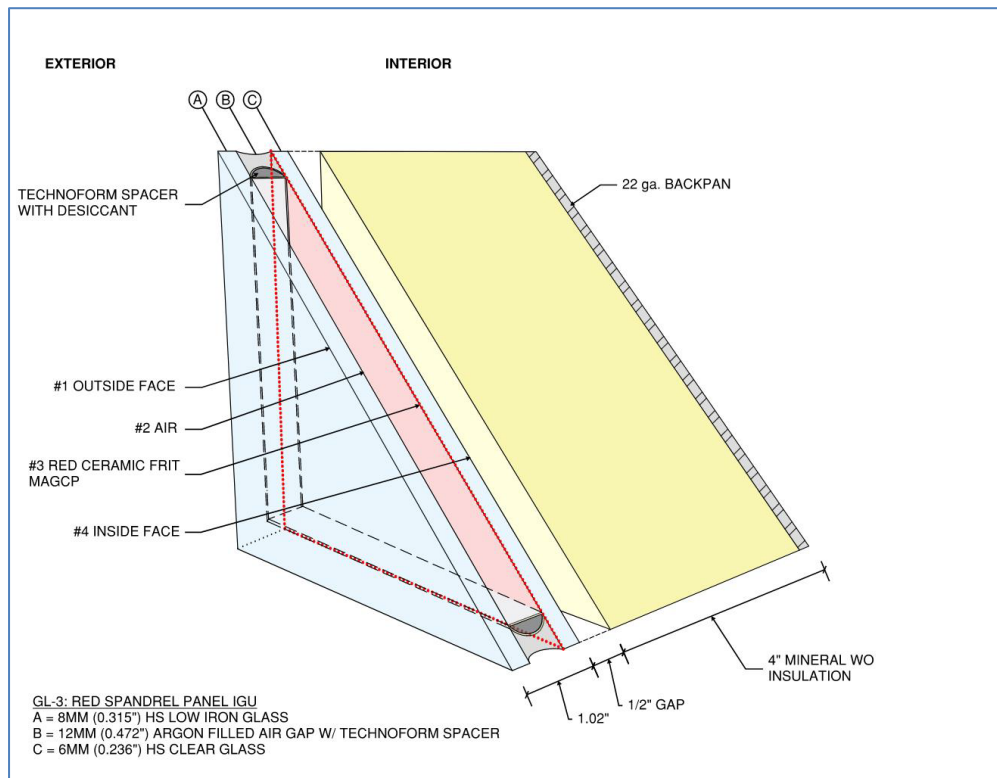


Fig. 1: Glass spandrel nomenclature (courtesy of Yashita Khanna and Terry McDonnell).

## 2. Mechanism of Thermal Fracture in Glass Panels

### 2.1. Griffith's flaws

When flat glass components for the spandrel panel are initially manufactured from raw materials, the resulting glass is annealed. One unavoidable physical trait of annealed glass is microscopic surface flaws, known as Griffith's flaws, that arise from tiny variations in the glass-cooling process. These tiny flaws will ultimately determine the conditions under which glass fractures (as well as a variety of other physical and chemical properties beyond the scope of this paper).

### 2.2. The Hot Environment

Thermal fracture can occur (usually near the perimeter of a glass spandrel panel) when the center of the glass exceeds the temperature of the edge of the same glass panel. The heat source is typically radiant energy from the sun.

Sunlight consists of three main portions: ultraviolet (shorter wavelength), visible, and infrared (longer wavelength). About 55% of sunlight is infrared, and about 42% is visible, making up the bulk of the light energy we consider when designing a window or spandrel panel.

The heat generated on the inner surface of the spandrel increases due to sunlight's physical interaction with the panel's material makeup. In particular, visible and infrared heat is either trapped in the airspace between surface No. 4 of the glass spandrel panel and the insulation or absorbed by the coating on the inboard glass panel surface. The darker the coating, the hotter the glass's interior surface. In addition, some low-e coatings contain metallic elements that absorb sunlight and convert that sunlight into heat.

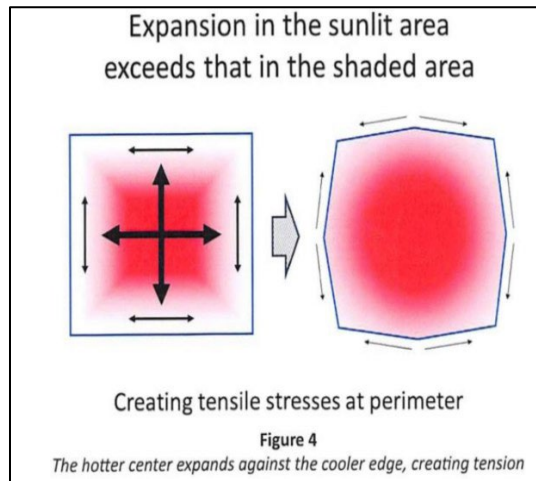


Fig. 2: From the free NGA Glass Technical Paper FB62-19; illustrating how temperature imbalance affects the differential expansion of glass.

### 2.3. Temperature Gradient on the Spandrel Panel

According to NGA Glass Technical Paper FB62-19 (National Glass Association, 2019), when an unbalanced temperature gradient develops across the surface of a glass panel, the glass deforms in response to the differential temperature gradient. Because the temperature is higher at the center vs. the edge, the center of the glass expands more than the edges, resulting in a stress zone near the perimeter of the glass where the temperature gradient is usually the most pronounced.

### 2.4. Heat Evolution in Spandrels vs. Vision Glass

This temperature differential is magnified by the insulated cavity within the spandrel assembly, and the coating located on the interior surface (see Figure 2) which has less opportunity to shed heat when compared to the typical face glass element, which benefits from a large volume of exterior air at ambient temperature. Exterior exposure helps vent and reduce the overall temperature differential across the glass surface. All glass elements should be analyzed for temperature effects; however, the authors' experience indicates that thermal fractures in face-glass elements are very rare and thus are not covered in this paper.

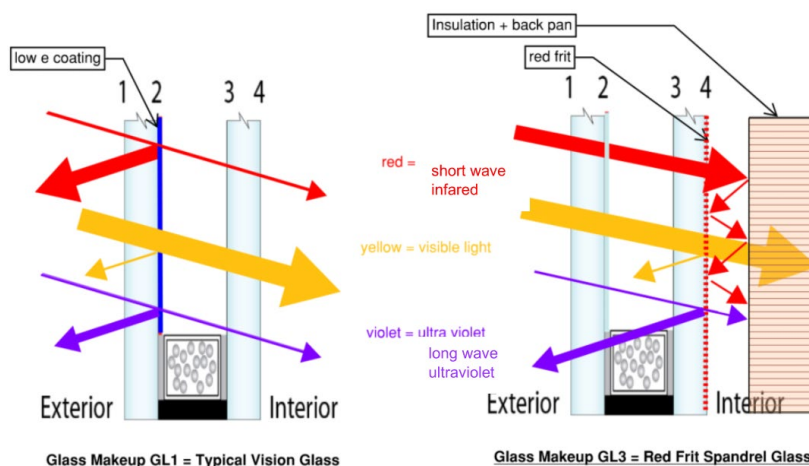


Fig. 3: Conceptual illustration of the interaction of sunlight with vision glass vs. spandrel panels with insulated backpan (courtesy of Terry McDonnell).

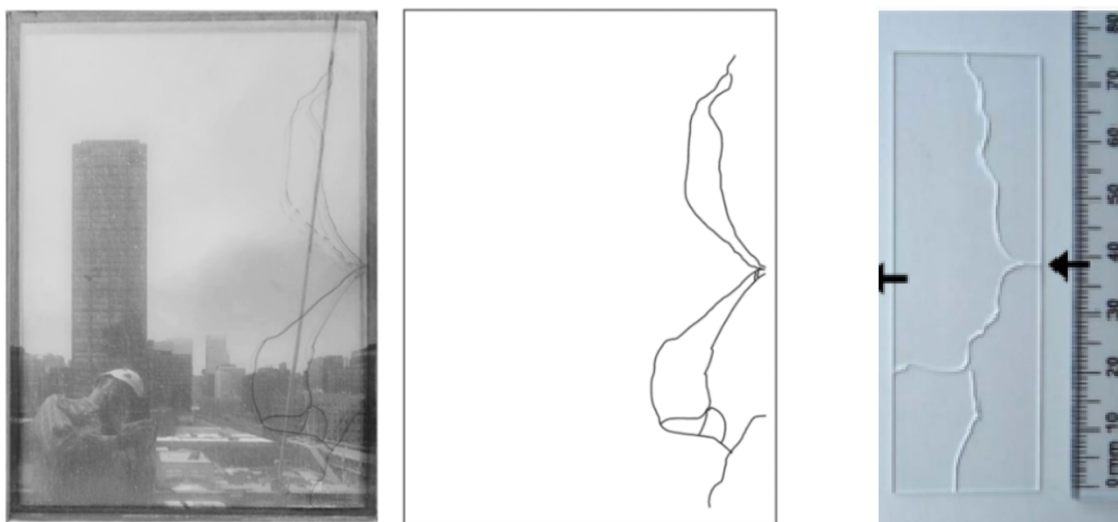
## 2.5. Glass Load Resistance

While it is entirely proper to consider the various glass type options for resisting differential temperature stress (such as heat-strengthened or fully tempered glass in lieu of annealed glass), the authors have experienced much more inconsistency in the determination and application of the differential temperature loads to spandrel panels, and thus, this paper focuses on the methodologies used to determine the temperature extremes at the center of glass and at the perimeter of the glass.

In general, the authors have not observed large discrepancies when applying this temperature differential. The minimum and maximum temperature values are commonly applied to resemble Figure 3, with the maximum temperature at the center of glass, and the minimum temperature applied around the perimeter of the glass.

## 2.6. Thermal Cracking Leaves Telltale Crack Patterns

As stated in the NIST recommended practice for fractography of glass (Quinn, 2016), “Certain types of fracture leave telltale fracture patterns on the fracture surfaces or have telltale breakage patterns or fragment shapes.” From the same resource, Quinn continues to show examples of telltale signs of temperature or thermal fractures. Both Quinn and National Glass Association FB62-19 describe thermal fractures of window panels that occur when the center of the glass is heated more than the edges, thereby creating differential strains: compression in the middle of the plate and tension at the rim or edges. The thermal crack commonly starts at or near the edge of the glass. The crack then propagates perpendicular to the edge before eventually changing direction into a meandering, wavy pattern as it approaches the biaxial compression stress near the center of the glass plate. NGA FB62-19 also describes the fracture of the spandrel, which frequently occurs on the inboard glass lite.



Photograph and sketch of fracture pattern in a typical spandrel panel (Courtesy Ron Spellish).

Typical thermal break in a glass sample shown in Quinn (2016).

Fig. 4: Fracture patterns observed at the Chicago case study and comparison to NIST handbook example (Quinn, 2016).

## 2.7. Code Requirements

The International Building Code (IBC) references the American Society of Civil Engineers (ASCE-7) for determining minimum loads and load combinations in the United States. ASCE 7-16 states within section 2.4.4 that those thermal stresses shall be considered when temperature or thermal changes

adversely affect an element's performance (i.e., load resistance). These stresses must be combined with other stresses (such as wind, seismic, and movement) to ensure adequate structural load resistance for the spandrel glass panel, consistent with the general reliability of all other building materials. For a vertically oriented spandrel panel, the most common load combinations are:

$$1.2D \pm 1.0 W + T \quad (1)$$

$$1.2D \pm 1.0 E + T \quad (2)$$

Where the load factor of (T) shall not have a value less than 1.0. For design purposes, T may represent the overall temperature differential between the center and edge of the glass that induces stress, depending on the limit state considered.

### 3. Differential Temperature Methodologies

In the following sections, various approaches considering differential temperature are discussed, highlighting the benefits and drawbacks for designers.

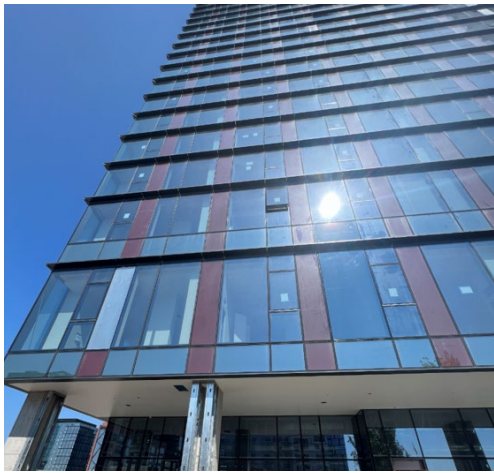
#### 3.1. Approach 1: Direct Measurements from Triano and Cocca Case Study (2012)

A handful of case studies on spandrel panel breakage where thermal cracking is a likely or suspected cause have been published. Triano and Cocca (2012) presented a case study from a 50-story residential tower in the northeastern USA. A recent case study, discussed later in this paper, also had a substantial number of spandrel glass units exhibiting fracture, while no fractures were reported on vision glass. A spandrel glass panel on the east elevation was instrumented with thermocouples at the center of the glass and at various locations on the No. 4 surface (closest to the building interior). Triano and Cocca reported a typical maximum temperature differential of 131°F (73°C) on a clear spring morning between the center and one of the edge sensors. The authors attributed this high temperature difference to differential exposure to sunlight as the sun rose: the center of the glass is fully exposed, while the edges remain shaded by the glazing pocket. The authors further noted that insulation batts installed between the No. 4 face and the interior of the tower were in contact with the glass, contrary to the design, which called for an air gap, thereby exacerbating solar heating of the spandrel glass.

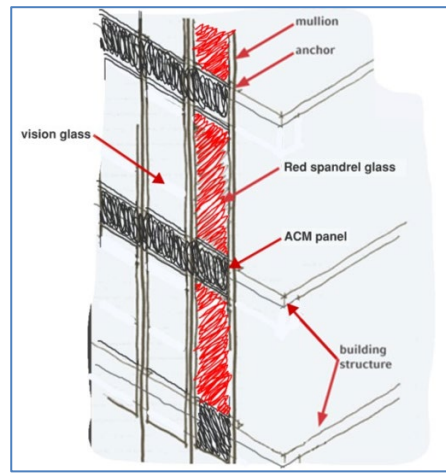
#### 3.2. Approach 2: Additional Case Study: Chicago (2023)

Temperature differentials have been better understood through forensic investigation of spandrel glass breakage. A 30-story residential structure in the Chicago area, with an exterior consisting of vision and spandrel glass, was recently investigated. An overall view of the subject building exterior and a conceptual diagram of the curtain wall components are shown in Figure 5 while the glass makeup and component thickness are shown in Figure 1.

Construction began in the spring of 2022, and broken glass was reported beginning in January 2023. Additional reports of broken glass were made in February, March, and April. A total of 150 glass spandrel panels had been reported as fractured by summer 2023. Fractured spandrel panels were observed on all elevations. All known fractures occurred on the inner layer of an IGU with an opaque coating on the No. 3 or No. 4 surface. The fracture patterns were consistent with thermal stress. Figure 5 shows a photograph and sketch of a typical fracture pattern from the subject building alongside a handbook example of thermal break in a glass sample.



(a) Building exterior showing vertical red spandrel panels (photo taken by Terry McDonnell).



(b) Conceptual sketch of curtain wall (Sketch by Terry McDonnell).

Fig. 5: Chicago case study, a 30-story residential building.

### 3.3. Chicago 2023 Monitoring Program

Two locations on a mid-level floor of the building were selected for monitoring: one east-facing and one west-facing. Self-adhesive thermocouples were applied directly to the No. 4 surface. A small access hole was cut into the insulation pan, and a “plug” of insulation was removed to allow installation of the thermocouples. Following installation, the insulation plug was reinstalled (taking care to preserve an air gap between the insulation and the glass), and the access hole was sealed with aluminum tape.



Fig. 6: Annotated photographs of instrumented spandrels in west- and east-facing units at the Chicago case study (photos by David Kosnik).

### 3.4. Chicago 2023 Monitoring Data and Observations

Unsurprisingly, the measured spandrel temperatures are strongly dependent upon sun exposure. Higher daily temperatures in the spandrel temperature time histories are strongly associated with sunny days, as indicated by cloud cover measurements from the automated weather station at Midway

Airport. Similar daily high glass temperatures occur on sunny days with considerably different air temperatures. For example, daily high glass temperatures approaching 200°F (93.3 °C) were recorded on the top thermocouple in the west-facing unit on days when the daily high air temperature was over 80°F (26.7 °C), as well as on days when it was below 60°F (15.6 °C).

The peak temperature differences for the east and west sides over the course of monitoring are summarized in Table 1. Figure 7 illustrates representative selections of  $\Delta T$  time histories for the east- and west-facing thermocouples over the entire monitoring period, also shown on the  $\Delta T$  time histories of the official air temperature at Chicago Midway Airport (Figure 7). It is noted that similar  $\Delta T$  values are observed during periods of different air temperatures. Examples in the data show  $\Delta T$  center–left for the west-facing unit on sunny days reached 70–80°F (38.8–44.4 °C) both in early September, when the daily high-low air temperatures were approximately 90/70°F (32.2/21.1 °C), and in late October, when the daily high-low air temperatures were approximately 45/60°F (7.2/15.6 °C).

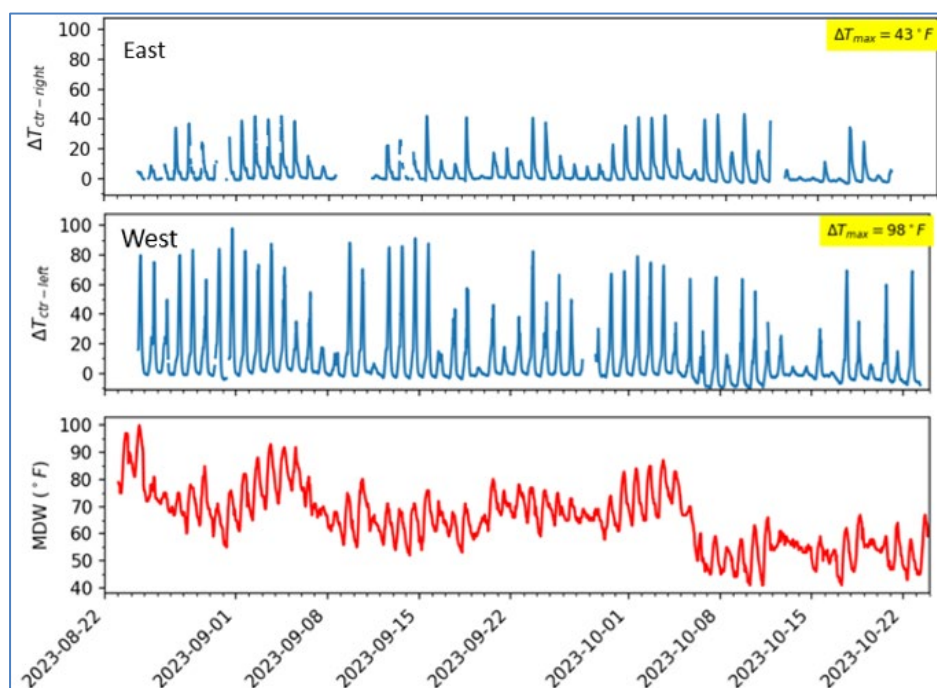


Fig. 7: Time histories of temperature differences  $\Delta T_{\text{center-right}}$  at east-facing unit and  $\Delta T_{\text{center-left}}$  at west-facing unit, and official air temperature at Chicago Midway Airport throughout the monitoring period.

Table 1: Peak  $\Delta T$  with respect to center of glass.

Exposure	Fahrenheit				Celsius			
	Top	Left	Right	Bottom	Top	Left	Right	Bottom
East	32	46	43	<b>79</b>	17.8	25.6	23.9	<b>43.9</b>
West	54	<b>98</b>	41	58	30	<b>54.4</b>	22.8	32.2

### 3.5. Extrapolation of Raw Data to Winter Temperatures and Unconditioned Space

Given that spandrel breakage was reported while the building interior was unconditioned in winter, a method was devised to extrapolate  $\Delta T$  values for an unconditioned space in winter from values

measured in a conditioned space in summer. A conceptual model was developed based upon glass and air temperatures recorded during the project, plus the following assumptions:

- The direct data provided for a  $\Delta T = 98^{\circ}\text{F}$  ( $54.4^{\circ}\text{C}$ ) during the summer (August through September) when the interior space is conditioned to approximately  $70^{\circ}\text{F}$  ( $21.1^{\circ}\text{C}$ ). For the unconditioned space, the authors assumed that both the center and the edge of the glass were at the same temperature just before dawn because the building was not yet fully enclosed and lacked a functioning heating system.
- We further presumed that the pre-dawn temperature was set to the overnight low air temperature reported at Midway Airport on February 3, 2023 ( $+2^{\circ}\text{F}$  or  $-16.7^{\circ}\text{C}$ ). The date is notable because it was one week before construction workers first observed spandrel fractures.
- Maximum heating of a glass over the course of the day is approximately  $186^{\circ}\text{F}$  ( $85.6^{\circ}\text{C}$ ) above the pre-dawn temperature, and this maximum value occurs approximately 2.5 hours after the sun's rays first reach the subject window [for the east-facing windows].
- For west-facing windows, substitute 1:30pm for dawn, as data showed that was when direct exposure to the sun's rays began.

The conceptual temperature evolution was developed to alter  $\Delta T=98^{\circ}\text{F}$  ( $54.4^{\circ}\text{C}$ ) as follows:

1. The authors created a heat transfer model of the spandrel panel jam using THERM, software developed by Lawrence Berkeley National Laboratory to model heat transfer through envelope systems.
2. The authors performed a parametric study using interior and exterior temperatures representative of the conditions present for an unconditioned space in wintertime (February).
  - A. THERM model interior:  $T(\text{interior}) = 70^{\circ}\text{F}(21.1^{\circ}\text{C})$  ;  $T(\text{exterior}) = 120^{\circ}\text{F}(48.9^{\circ}\text{C})$ ;  $\Delta T(\text{int}) = 5.5^{\circ}\text{F}(3.1^{\circ}\text{C})$
  - B. THERM model exterior:  $T(\text{interior}) = 0^{\circ}\text{F}(-17.8^{\circ}\text{C})$  ;  $T(\text{exterior}) = 120^{\circ}\text{F}(48.9^{\circ}\text{C})$ ;  $\Delta T(\text{ext}) = 11^{\circ}\text{F}(6.1^{\circ}\text{C})$

In addition, the authors measured the  $\Delta T$  difference in temperature from the placement location of the thermal couple to the actual glass edge in the conditioned THERM model. The difference was  $28^{\circ}\text{F}(15.6^{\circ}\text{C})$ . The THERM model was calibrated to match the reading of the thermal couple at its distance from the edge of the metal frame. However, we were unable to measure the temperature at the edge of the metal frame due to access constraints.

1. The Tedge value for the conceptual temperature evolution curve was reduced
2. Fit a third-degree polynomial to the Tcenter and Tedge time histories from the representative sunny day (Figure 8)
3. Iteratively adjust the polynomial coefficients such that the above-listed givens are satisfied while the general shapes of the Tcenter and Tedge time histories are preserved.
  - A. The difference between the Tedge maximum and minimum values on the conceptual curve was increased by  $28^{\circ}\text{F}(15.6^{\circ}\text{C})$  to account for the instrumentation shift.
  - B. The difference between Tcenter and Tedge conceptual time histories was increased by 200% to account for the unconditioned winter scenario.
4. Calculate the conceptual  $\Delta T$  time history based upon the conceptual lot, the Tcenter, and Tedge time histories, and identify the time of maximum  $\Delta T$ .

The resulting conceptual model for unconditioned behavior on the coldest day of winter is shown in Figure 9.

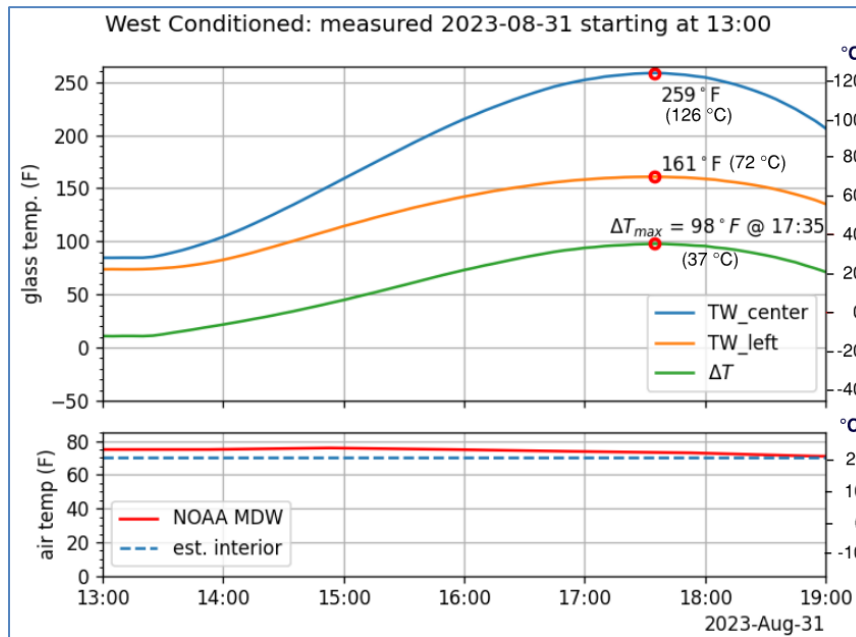


Fig. 8: West-side center and edge (left) temperature and temperature difference as measured in a west-facing conditioned space in August.

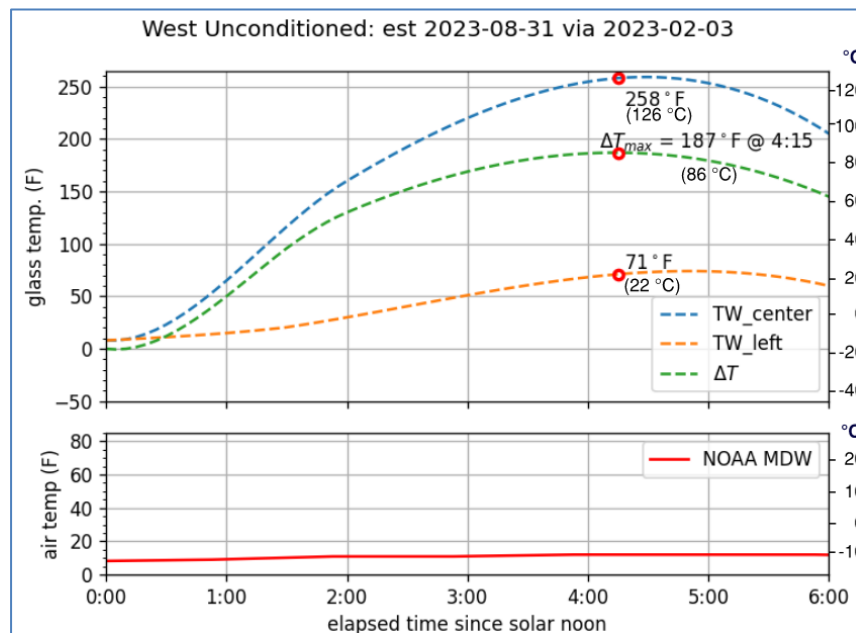


Fig. 9: Conceptual model of west-side center and edge (left) temperature for unconditioned space in February (overnight low +2°F or -16.7°C)

### 3.6. Approach 3: Rules of Thumb from NGA (2019)

The document NGA Glass Technical Paper FB62-19 is based on the report of Triano and Cocca (2012) describing glass spandrel fractures observed in a high-rise building in the northeastern USA. Data obtained from measuring temperatures directly on the No. 4 (innermost) glass surface indicated a maximum temperature difference of 130°F(72.2°C) between the center and edge of the glass. Notably, these measurements were taken in April, whereas similar data from August show a much smaller temperature differential. Also of note is that the data collection period did not extend through the

winter months and occurred while the interior space was temperature-controlled; extrapolation to cold weather or to situations where the interior spaces are unconditioned may warrant additional engineering judgment.

In addition, NGA FB62-19 lays out a correlation that “for every one degree of Fahrenheit differential between the center and edge of glass, a 50 psi-pounds per square inch (0.34 MPa) stress occurs within the innermost layer of glass. This “rule of thumb” makes accounting for temperature differential and thus calculating temperature-induced stress quite efficient for the designer to include within a design.

### 3.7. Approach 4: Numerical Method Utilizing Climate Records: Barry and Norville (2015)

This article described unanticipated fractures of spandrel glass and presented an implementation of the finite-difference method for estimating thermal stresses using spreadsheet macros. The authors suggested that the  $\Delta T$  is often greater than or equal to 212°F(117.8°C) for design purposes. The paper also discussed that using ceramic frit as an opaque coating can reduce the load resistance of glass.

### 3.8. Approach 5: Numerical Method Utilizing Climate Records: Montali, Laffranchini, and Micono (2020)

The article explains the maximum temperature difference at a location by first using hour-by-hour weather data and a one-dimensional steady-state heat-transfer model. The researchers downloaded hourly datasets covering all 8,760 hours of an entire year and used energy models programmed within the Integrated Environmental Solutions Virtual Environment (IESVE) version 2015 with the following data in order to create the boundary conditions for the temperature analysis.

- Outdoor air temperature ( $T_{ext}$ )
- Direct solar irradiance ( $I_{dir}$ )
- Diffuse solar irradiance ( $I_{diff}$ )

For each hour, they calculated the temperature at the sunlit center and the shaded perimeter of the glass. To do this, they applied a steady-state heat balance, which means they assumed temperatures were constant at each moment and did not accumulate heat over time. The matrix system of equations eventually sums the heat entering the glass from sunlight and balances it against the heat leaving the glass by conduction (heat moving through materials), convection (heat moving into the air), and radiation (heat emitted as energy). This process provides two temperatures per hour, and the temperature difference ( $\Delta T$ ) is calculated by subtracting the perimeter/shaded temperature from the sunlit temperature.

After calculating and checking all hourly temperature differences, the researchers used statistical methods (specifically a finite-difference / thermal-network system of linear equations (represented graphically by a set of springs in parallel and in series) to identify the maximum plausible temperature difference within a glass assembly for a specific geographic location (e.g. New York City). Once, the largest temperature differences the glass might experience were identified using probability theory; these values were plugged into a simple formula that relates temperature difference to thermal stress, helping engineers predict whether the glass could crack due to thermal shock.

Before performing the thermal stress calculations, the ( $\Delta T$ ) calculation curves are checked in SAS (Statistical Analysis System) software version 9.4, a data and AI tool developed by SAS Institute to perform statistical and error analyses of data sets with three or more varying contributions. The results from the curves are listed in the summary table (Table 2).

### 3.9. Approach 6: Simplified Calculation Utilizing Climate Records: Colvin and Lightfoot (1974)

The method, also known as the Pilkington method, was refined by Pilkington over the next 30 years into a simplified approach for determining temperatures used in thermal analysis of window glass. The method is based on the following equation:

$$\sigma = E \cdot \alpha \cdot \Delta T \quad (3)$$

- $E$  = Young's modulus of glass (ksi or )
- $\alpha$  = Coefficient of thermal expansion of glass (unitless)
- $\Delta T = T_{\text{center}} - T_{\text{edge}}$

$$\text{Where } \Delta T_{\text{center}} = q_{\text{abs}} / h_{\text{total}} = \text{°F} \quad (4)$$

- $q_{\text{abs}}$  = Solar radiation of the season in question (Btu/hr·ft<sup>2</sup> or W/m<sup>2</sup>) x Absorptance coefficient of the glass surface in question = (Btu/hr·ft<sup>2</sup> or W/m<sup>2</sup>)
- $h_{\text{total}}$  = Coefficient of thermal expansion of glass (unitless) =  $h_o + h_i$
- $h_o$  = Exterior heat transfer coefficient (unitless)
- $h_i$  = Interior heat transfer coefficient (unitless)

The  $T_{\text{center}}$  term relies on heat transfer coefficients that are tabulated for only a select few environmental conditions (average of summer, fall, winter, and spring), as well as tabulated values for solar radiation absorbed by the glass surface for the direction the glass faces. In addition, only a few major cities have these values tabulated.

Finally, the method explicitly states that the  $T_{\text{edge}}$  is presumed to only be slightly lower in temperature than the  $T_{\text{center}}$ . From the research, all examples the authors found using this method show  $\Delta T$  in the range of 9-36 °F (5-10 °C). We know from direct measurement approaches that this is simply inaccurate in many instances.

### 3.10. Approach 7: Simplified: Saint-GoBain reference to IStructE draft (2006)

The method published by Saint-Gobain (Saint-GoBain IABSE/IStructE draft, 2006) in one of their technical manuals, uses the basic John Colvin equation (3) listed above to back-calculate an allowable or maximum  $\Delta T$  based on the allowable edge stresses for various glass types (annealed, heat-strengthened, and fully tempered). The results are summarized in Table 2.

### 3.11. Approach 8: Numerical Method based on the French NF DTU 39 P3 (2006)

This French standard is purported to be widely used within the EU for determining thermal stresses arising from the temperature differential between the center and edge of the glass. For an insulated glass unit, this method uses a series of equations that represent heat flux through the insulated unit, and it can be used for both double and triple-pane insulated units.

The heat flux calculations use a simplified time-step heat-transfer model similar to that described in Montali, Laffranchini, and Micono (2020). The method uses a finite difference technique under transient conditions, where the intrinsic thermal resistance of the glass is neglected. For a number ( $n$ ) of components (glass lites and air spaces), the method consists of evaluating, for each component, the values of solar flux transmitted toward the interior, reflected toward the exterior, and absorbed by the component.

The  $\Delta T$  value of the exterior surface is largely determined by the initial temperature conditions found in climate temperature maps of France, as specified in the standard.

## 4. Discussion and Conclusions

The eight approaches considered herein vary in complexity, suitability for use in a production environment at a design firm (i.e., the balance of simplicity and accuracy), and reliance on direct data acquisition at the subject site versus the use of publicly available weather/climate records. Rules of thumb and approaches that employ readily available archival data are advantageous because no instrumentation is required. Rule-of-thumb approaches do not require computational modeling and are easier to understand and thus to review in design checks.

The governing temperature difference used within load combinations for examples of all methodologies described herein are summarized in Table 2, with the exception of the French NF DTU 39 P3. The French model does not include a result in this paper because it relies on initial temperatures from French climate data. For the United States, suitable substitutes for the initial maximum and minimum surface temperatures can be found in ASHRAE climate databases or in AASHTO v2016 Figures 3.12.2.2-4, which includes maps of 50-year temperature differentials for exposed structural materials.

Table 2: Summary of  $\Delta T$  for various spandrel glass temperature analysis methodologies and geographical locations.

Approach	Case Study	$\Delta T$ (°F/°C)	Location
Direct measurements	Triano and Cocca (2012)	131/72.8	Northeast USA
Direct measurements	Authors - Chicago (2023)	187/103.9	Chicago
Rule of Thumb	NGA FB62-19 (2019)	130/72.2	Sites throughout USA
Numerical based on weather records	Barry and Norville (2015)	212/117.8 (min.)	Sites throughout USA and Canada
		184/102	New York
Numerical based on weather records	Montali, Laffranchini, Micono (2020)	171/95	London
			Mumbai
		97/54	
Simple Calculation based on estimated Meteorological Data	John Colvin method (2004)	9-36/5-10	Sites throughout USA
Simple Calculation based on allowable edge stresses	IStructE / St. GoBain (2018)	81/45 (max) 180/100 (max) 360/200 (max)	EU float glass < 15mm Heat Strengthened Fully Tempered
Numerical based on weather records	French NF DTU 39 P3 (2006)	NA	NA

For practical design methodologies, the NGA FB62-19 is the most time-efficient; however, it is based on raw data, similar to the authors', and on summertime and conditioned space. The authors' case study shows that the NGA FB62-19  $\Delta T$  recommendation is too low for use as a generic case. Numerical methods summarized herein support the author's opinion that  $\Delta T = 130$  F is too low for designers to use as a generic load case.

In addition, direct measurements, the French time-step method, and the Montali, Laffranchini, and Micono numerical method are simply too time-consuming and impractical to incorporate into a general design methodology, even though their results are much closer to the minimum magnitude required to minimize glass breakage and take into account the local climate effects.

Of all the options, we hypothesize that the Barry and Norville Excel-based finite-difference method, using readily available climate data to graph the Tcenter and Tedge temperature vs. time curves, appears to offer a good balance of achieving a project-specific minimum  $\Delta T$  that is both efficient for a designer and provides large enough values that may be positively verified through independent testing.

## References

- ASCE/SEI 7-16: Minimum Design Loads and Associated Criteria for Buildings and Other Structures. American Society of Civil Engineers, Reston, Virginia.
- Barry, C., & Norville, H. S. (2015). "Unexpected Breakage in Ceramic Enamelled (Frit) HS IG Spandrels". In Proceedings, Insulating Glass Manufacturer's Alliance Winter Conference (Vol. 11).
- Colvin, J.B. and Lightfoot, D.G., Thermal Stress in Non-rectangular Glazing . Report No. 382, Technical Sales Laboratory, Pilkington, 1974.
- French Standard (2006). NF DTU 39 P3. Building Works, Glazing and Mirror Work, Part 3: Handbook of thermal stress calculations.
- Haldimann, M., Luible, A., & Overend, M. (2008). Structural Use of Glass. IABSE
- Montali, J., Laffranchini, L., & Micono, C. (2020). Early-Stage Temperature Gradients in Glazed Spandrels Due to Aesthetical Features to Support Design for Thermal Shock. Buildings, 10(5), 80. <https://doi.org/10.3390/buildings10050080>
- National Fenestration Rating Council. (2011). NFRC 100: Procedure for Determining Fenestration Product U-factors.
- National Glass Association (2019) "Thermal Stress in Heat-Treated Spandrel Glass". Glass Technical Paper FB62-19.
- Quinn, G. D. (2016). Fractography of Ceramics and Glasses. NIST Recommended Practice Guides / Special Publication 960-16e2. National Institute of Standards and Technology, US Dept. of Commerce. 640 pp. <http://dx.doi.org/10.6028/NIST.SP.960-16e2>
- Saint-GoBain (2006). Thermal Safety 3A: The Resistance of Glass to Thermal Stress. Saint-GoBain Building Glass, UK and Ireland.
- Triano, J. & Cocca, J. (2012). "Thermal Breakage of Spandrel Glass: A Case Study". In Proceedings, Forensic Engineering 2012 (pp. 143-150). American Society of Civil Engineers, Reston, Virginia.

## Platinum Sponsor

---



## Gold Sponsors

---



## Silver Sponsors

---



## Organisation

---

